Influence of magnetic anisotropy on hysteresis behavior in the two-spin model of a ferro/antiferromagnet bilayer with exchange bias

Cite as: Low Temp. Phys. **38**, 937 (2012); https://doi.org/10.1063/1.4758774
Published Online: 01 November 2012

A. G. Grechnev, A. S. Kovalev, and M. L. Pankratova

Influence of magnetic anisotropy on hysteresis behavior in the two-spin model of a ferro/antiferromagnet bilayer with exchange bias

A. G. Grechnev, A. S. Kovalev, and M. L. Pankratova[a)]

B. Verkin Institute for Low Temperature Physics and Engineering of the National Academy of Sciences of Ukraine, 47 Lenin Ave., Kharkov 61103, Ukraine
(Submitted May 21, 2012)
Fiz. Nizk. Temp. **38**, 1184–1190 (October 2012)

The influence of magnetic anisotropy of a ferromagnetic film on the phenomenon of exchange bias is studied here. Hysteresis behavior in the two-spin model of a ferro/antiferromagnetic (FM/AFM) bilayer with exchange bias has been investigated in detail. In this model a half-space of an AFM with fixed magnetic configuration comes in contact with a two-layer FM film. Twelve different types of magnetization curves $M(H)$ (both with and without hysteresis) have been found. Some of the $M(H)$ curves demonstrate unusual features, such as plateaus and inclined segments. The hysteresis loop becomes asymmetric if surface anisotropy is taken into account. © *2012 American Institute of Physics*. [http://dx.doi.org/10.1063/1.4758774]

Introduction

Layered ferro/antiferromagnetic (FM/AFM) systems are important objects for the read/write heads of modern data storage devices. They demonstrate the exchange bias effect,[1–3] which takes place in the shift of the hysteresis loop from the $H=0$ position: $\mathbf{M}(\mathbf{H}) \neq -\mathbf{M}(-\mathbf{H})$ after field cooling. At the same time, coercivity is increased greatly. In recent experiments[4,5] asymmetric hysteresis loops, inclined segments of the $\mathbf{M}=\mathbf{M}(\mathbf{H})$ curves, and horizontal plateaus (steps) in the $M(H)$ curves were observed. This complicated behavior is not caused by the kinetics of magnetization reversal (by the finite rate of field change in the experiment), but is apparently caused by certain nonuniform and noncolinear (canted) states of the magnetic layers. This correlates with the fact that all modern theories of the exchange bias phenomenon[6–10] involve nonuniform states (domain walls or incomplete domain walls) and/or interface roughness to explain many peculiar features of this phenomenon.

In our previous works[11,12] two simple theoretical models of the FM/AFM bilayer with exchange bias (the "two-spin model" and the "continuous model") were proposed. In particular, the two-spin model is the simplest possible model, which allows nonuniform magnetic states. Despite simplicity, it can qualitatively explain many features of the exchange bias phenomenon. All possible magnetic structures of the two-spin model were found in Ref. 11; however, the detailed study of the hysteresis phenomenon was beyond the scope of the previous paper. The properties of the domain walls in a bilayer FM/AFM system with imperfect interface and their connection with the exchange bias phenomenon were discussed in Ref. 13.

The goal of the present paper is to determine all possible types of the $M(H)$ curves (all shapes of the hysteresis loops and the magnetization reversal without hysteresis), which arise in the two-spin model. This paper is organized as follows. Chapter 1 defines the two-spin model. Chapter 2 examines the regions of stability of different collinear phases and presents the mechanism of the onset of hysteresis. Chapter 3 lists all types of $M(H)$ curves and defines the corresponding regions in the plane defined by the system parameters. Chapter 4 examines the hysteresis in the two-spin model in yet more detail. Chapter 5 briefly examines the case where the anisotropy constants are different for two FM layers (which simulates surface anisotropy). Chapter 5 is followed by the conclusion.

1. Model

The present paper uses the two-spin model introduced in Ref. 11. Consider a FM/AFM bilayer consisting of a magnetic hard AFM subsystem, in which all magnetic moments are fixed and do not rotate during field reversal, and a FM subsystem consisting of two magnetic layers. (In Ref. 12 it was demonstrated that many features of field dependencies of magnetization in the two-layer model and the continuous model of thin FM layer are the same after renormalization of exchange interaction constants. On the other hand, perhaps the two-layer system represents a particular case pertaining to the problem. In any case this model can be used for the description of real two-layer films studied experimentally.) The magnetic state is determined by the rotation angles φ_i of the magnetization vectors in the easy plane. In addition, a weak easy-axis anisotropy in this plane is taken into account. It is also assumed that the external magnetic field is directed along the easy axis. The magnetic state of the system is assumed to be uniform along the interface. The energy of the systems is

$$E = -J_0 \cos\varphi_1 - J\cos(\varphi_1 - \varphi_2) - \frac{\beta_1}{2}\cos^2\varphi_1 - \frac{\beta_2}{2}\cos^2\varphi_2 - H(\cos\varphi_1 + \cos\varphi_2), \quad (1)$$

where J_0 represents the exchange interaction across the interface (FM–AFM exchange, assumed to be ferromagnetic), J is the exchange interaction between two FM layers, β_i are the anisotropy constants for the two FM layers, and H is the external magnetic field. Indices 1 and 2 correspond to the layer adjacent to the interface and the second FM layer (on the free boundary of the FM), respectively. The possible equilibrium states are given by the equations $\partial E/\partial\varphi_i = 0$, $i = 1, 2$, namely:

$$(H+J_0)\sin\varphi_1+J\sin(\varphi_1-\varphi_2)+\beta_1\sin\varphi_1\cos\varphi_1=0, \quad (2)$$

$$H\sin\varphi_2+J\sin(\varphi_2-\varphi_1)+\beta_2\sin\varphi_2\cos\varphi_2=0. \quad (3)$$

First we note that the collinear structures (↑↑ and ↓↓ phases, $\varphi_1=\varphi_2=0,\ \pi$) with vectors $\mathbf{M}_i$ parallel to each other and parallel or antiparallel to the direction of the magnetic field, respectively, are solutions of Eqs. (2) and (3). The solutions with antiparallel directions of the vectors $\mathbf{M}_i$ (↑↓ and ↓↑ phases) also exist. In Secs. 1–4, we consider the case of equal anisotropy constants for the two FM layers: $\beta_1=\beta_2=\beta$ (the case $\beta_1\neq\beta_2$ is studied in Sec. 5). Upon certain conditions there also exists a canted (noncollinear) solution of Eqs. (2) and (3) with $\varphi_i\neq 0,\ \pi$. This is the two-spin equivalent of the "incomplete domain wall" object discussed in the exchange bias literature. In the presence of anisotropy (even for $\beta_1=\beta_2$) the canted solutions $\varphi_i=\varphi_i(H)$ cannot be found analytically. It is easy to show that the magnetization curve $M(H)$ for $\beta_1=\beta_2$ is antisymmetric with respect to the exchange bias field $H=-J_0/2$. (Energy (1) is invariant under the transformation $\phi_i\to\pi-\phi_i$, $H\to -J_0-H$.) The hysteresis loop possessing this symmetry is called "symmetric hysteresis loop" in the exchange bias literature, and the opposite is the "asymmetric hysteresis loop" (see Sec. 5).

2. The boundaries of the hysteresis loop

In our previous work[11] the transformation of the collinear ↑↑ phase ($\varphi_1=\varphi_2=0$) to the canted phase was considered. This transition corresponds to the bifurcation of the solution $\varphi_1=\varphi_2=0$. In vicinity of the bifurcation point there are canted solutions of Eqs. (2) and (3) that are infinitesimally close to the collinear phase. In order to find this point we linearize Eqs. (2) and (3) with respect to the angles φ_i and look for the nonzero solutions of the linearized equations. This gives the bifurcation field

$$H_{\uparrow\uparrow}=\left(\sqrt{J_0^2+4J^2}-(J_0+2J)\right)\Big/2-\beta. \quad (4)$$

It is marked in Fig. 1 as point (a).

In the absence of hysteresis (see below) the ↑↑ phase is stable for $H>H_{\uparrow\uparrow}$, while for $H<H_{\uparrow\uparrow}$ the canted phase is stable. When hysteresis is present, however (as shown in Fig. 1),

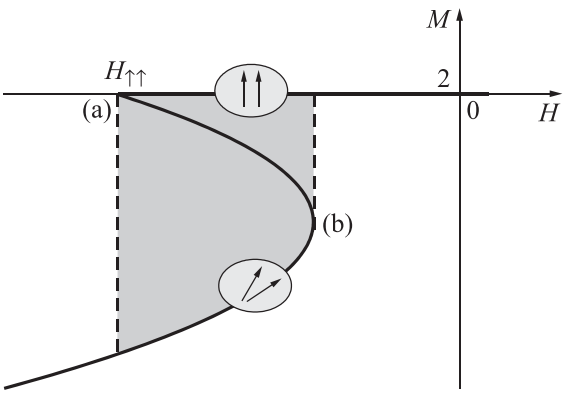

FIG. 1. Transformation of the collinear ↑↑ phase into the canted phase: (a)—bifurcation point, (b)—the point with $dM/dH=\infty$. The hysteresis loop is filled.

$H_{\uparrow\uparrow}$ gives the lower boundary on the hysteresis loop, and the canted phase is stable even for $H>H_{\uparrow\uparrow}$.

The dynamical stability of any given structure (collinear or canted) is determined by the Hessian of the potential energy surface $E=E(\varphi_1,\varphi_2)$, i.e.,

$$K=\frac{\partial^2E}{\partial\varphi_1^2}\frac{\partial^2E}{\partial\varphi_2^2}-\left(\frac{\partial^2H}{\partial\varphi_1\partial\varphi_2}\right)^2. \quad (5)$$

The structure in question is stable for $K>0$, which corresponds to the minimum of potential energy. At the saddle point of potential energy surface ($K=0$) the structure loses stability. For the collinear ↑↑ phase

$$K=(H+\beta)(H+J_0+\beta)+J(2H+J_0+2\beta), \quad (6)$$

and, by comparing with Eq. (4), we obtain the expected result that it loses stability exactly at the bifurcation point.

Analysis of the stability of the ↓↓ phase ($\varphi_{1,2}=\pi$) can be done in a similar way, and the result is

$$H_{\downarrow\downarrow}=\left(-\sqrt{J_0^2+4J^2}+2J_0-J_0\right)\Big/2+\beta. \quad (7)$$

The antiparallel phase ↑↓ ($\varphi_1=0$, $\varphi_2=\pi$) corresponds to the plateau (a region with $M=$const, or, more specifically, $M=0$ in this case) in the field dependence of magnetization $M(H)$. Another possible antiparallel phase, ↓↑ ($\varphi_1=\pi$, $\varphi_2=0$) always has higher energy compared to the ↑↓ phase (for $J_0>0$), and therefore it is not important for the present paper. The antiparallel phases lose stability at

$$H_{\uparrow\downarrow}=-J_0/2\pm\sqrt{(J_0/2-J+\beta)^2-J^2}. \quad (8)$$

Equation (4) determines one of the boundaries of the hysteresis loop (or, in general, the region of magnetization reversal) in the H axis. As will be shown below, for small enough anisotropy there is no hysteresis, and magnetization switches via the uniform magnetization reversal process through a region of the canted phase. It roughly corresponds to the picture of both spins rotating as one with the change of H, with the angle $\varphi_1-\varphi_2$ between two spins being rather small. The ↑↑-canted phase transition is of the second order in this case.

Hysteresis appears when the derivative dM/dH for the canted phase becomes negative at the bifurcation point (see Fig. 1). To determine the critical values of the parameters for which the hysteresis appears ($dM/dH=\infty$), we find the slope of the $M(H)$ curve in the canted phase near the bifurcation point. To do this, we expand the Eqs. (2) and (3) into a series with respect to the variables φ_i up to cubic terms:

$$(H+J_0+J+\beta)\varphi_1-J\varphi_2-\frac{1}{6}(H+J_0+4\beta)\varphi_1^3 -\frac{J}{6}(\varphi_1-\varphi_2)^3=0, \quad (9)$$

$$(H+J+\beta)\varphi_2-J\varphi_1-\frac{J}{6}(H+4\beta)\varphi_2^3+\frac{J}{6}(\varphi_1-\varphi_2)^3=0, \quad (10)$$

and look for the solutions in the form of power series with respect to small deviations of the magnetic field from its bifurcation value $\varepsilon = \sqrt{H - H_{\uparrow\uparrow}}$: $\varphi_i \approx \varphi_i^{(0)}\varepsilon + \varphi_i^{(1)}\varepsilon^3 + \ldots$. In the first order in ε we obtain the bifurcation field and the relation between the amplitudes of the two angles:

$$\varphi_2 \approx \varphi_1(J_0 + J_1)/2J, \tag{11}$$

where $J_1 = \sqrt{J_0^2 + 4J^2}$. In the third order in ε we obtain the values of the angles $\varphi_{1,2}$:

$$\varphi_{1,2}^2 \approx \frac{\varepsilon^2 J_1(J_1 \mp J_0)}{\beta(J_0^2 + 2J^2) - J^2(J_1 - 2J)}. \tag{12}$$

The dependence of magnetization of the system on the magnetic field near the bifurcation point is given by the formula

$$M(H) \approx 2 - (H - H_{\uparrow\uparrow})\frac{J_1^2}{\beta(J_0^2 + 2J^2) - J^2(J_1 - 2J)}. \tag{13}$$

For the given values of parameters J and J_0, hysteresis appears for the critical value of the anisotropy parameter:

$$\beta_{c1} = J^2\frac{J_1 - 2J}{J_0^2 + 2J^2}. \tag{14}$$

There is no hysteresis for $\beta < \beta_{c1}$. This is in qualitative agreement with the experiment: for different systems with exchange bias, both uniform magnetization reversal and hysteresis are observed.

3. Dependence of the shape of the hysteresis on the anisotropy parameter

In this section we analyze and classify all possible types of the $M(H)$ dependence (both with and without hysteresis), which arise in the model of Sec. 1 for different values of anisotropy parameter β/J and FM–AFM exchange parameter J_0/J. A numerical solution of Eqs. (2) and (3) was obtained by a relaxation algorithm. Namely, a (local) minimum of the total energy (1) is found by solving the system of differential equations $\partial\varphi_i/\partial t = -\partial E/\partial\varphi_i$ ($i = 1, 2$) numerically, which is done by the iterative procedure $\varphi_i \to \varphi_i - \varepsilon\,\partial E/\partial\varphi_i$, where ε is a sufficiently small parameter. Magnetization curves $M(H)$ corresponding to several characteristic values Z_i of the exchange interaction and anisotropy are depicted in Fig. 2. Points Z_i in the (β/J, J_0/J) plane are presented in Fig. 3. In general there can be more than one local minimum of the energy $E(\varphi_i)$, which results in hysteresis behavior. These minima can be found by starting the relaxation algorithm from different initial values of φ_i. To simulate the hysteresis, we ran the relaxation algorithm twice for each point Z_i and for each value of H, starting in vicinity of the collinear phases $\uparrow\uparrow$ and $\downarrow\downarrow$, respectively (solid curves in Fig. 2). In addition, when appropriate, we started in vicinity of the $\uparrow\downarrow$ phase, which sometimes gives new energy minima (dashed curves in Fig. 2).

In total, twelve different types of the $M(H)$ dependence were found. They correspond to twelve different regions in the (β/J, J_0/J) plane (Fig. 3). For each region, one point Z_i was chosen arbitrarily. The regions are separated by the curves $\beta_{ci}(J_0/J)$, $i = 1,\ldots, 5$ in Fig. 3. The expressions for $\beta_{c1}\ldots\beta_{c4}$ were found analytically (and verified by numerical

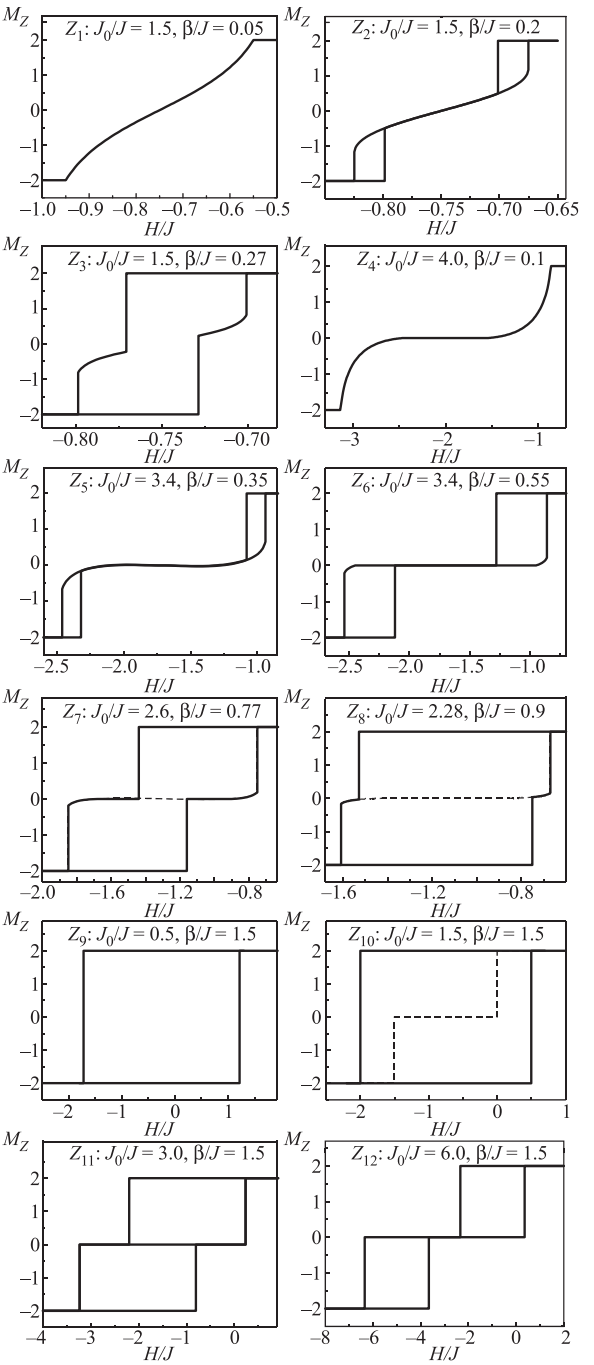

FIG. 2. Different shapes of the $M(H)$ hysteresis loop for different values of magnetic anisotropy β/J and the FM–AFM exchange parameter J_0/J.

simulations), while the curve $\beta_{c5}(J_0/J)$ was obtained numerically. Equation (14) gives the expression for the critical value β_{c1} of anisotropy, for which hysteresis appears. For $\beta < \beta_{c1}$ there is no hysteresis (Fig. 2, points Z_1, Z_4). The second critical value of anisotropy

$$\beta_{c2} = 1/2\left(\sqrt{4J^2 + J_0^2} - 2J\right)$$

is obtained from the condition $H_{\uparrow\uparrow} = H_{\downarrow\downarrow}$, where the expressions for $H_{\uparrow\uparrow}$, $H_{\downarrow\downarrow}$ are given by Eqs. (4) and (7). For $\beta > \beta_{c2}$ there is a region of H for which both collinear phases ($\uparrow\uparrow$ and $\downarrow\downarrow$) are dynamically stable. For $\beta_{c1} < \beta < \beta_{c2}$ there are two hysteresis loops separated by a region of the canted phase or the $\uparrow\downarrow$ phase (Fig. 2, points Z_2, Z_5, Z_6, Z_{12}). For

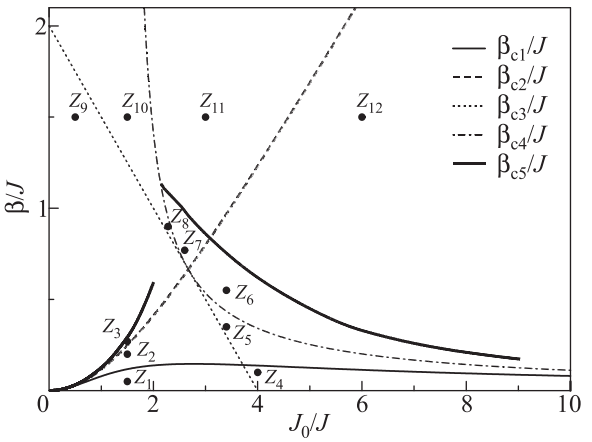

FIG. 3. Different types of the $M(H)$ dependence in the plane of the parameters $(\beta/J, J_0/J)$.

$\beta > \beta_{c2}$, however, there is a single hysteresis loop (Fig. 2, points Z_3, $Z_7 - Z_{11}$). The third critical anisotropy β_{c3} corresponds to the appearance of the $M = 0$ plateau (the $\uparrow\downarrow$ phase). For $\beta > \beta_{c3}$ there is a $M = 0$ plateau in the $M(H)$ curve (Fig. 2, points $Z_5 - Z_8$, $Z_{10} - Z_{12}$). From the condition $H_{\uparrow\downarrow} = -J_0/2$, where $H_{\uparrow\downarrow}$ is given by Eq. (8), we obtain $\beta_{c3} = 2J - J_0/2$. The fourth critical anisotropy β_{c4} corresponds to the coexistence of the collinear phases $\uparrow\uparrow$ (or $\downarrow\downarrow$) and $\uparrow\downarrow$. For $\beta_{c3} < \beta < \beta_{c4}$ the $\uparrow\downarrow$ phase only appears in the middle of the region of the canted phase (Fig. 2, points Z_5, Z_8) or inside the hysteresis loop (Fig. 2, point Z_{10}). For $\beta > \beta_{c4}$ (Fig. 2, points Z_6, Z_7, Z_{11}, Z_{12}) the $\uparrow\downarrow$ phase takes part in the formation of the hysteresis loop(s). The value of β_{c4} can be determined from the condition $H_{\uparrow\uparrow} = H_{\uparrow\downarrow}$, where $H_{\uparrow\downarrow}$ is given by Eq. (8). It is given by the implicit expression

$$J_0 = \frac{\beta + J}{2\beta}\left(J + \sqrt{J^2 + 4\beta^2}\right) - \beta.$$

Finally, for $\beta > \beta_{c5}$ (Fig. 2, points $Z_9 - Z_{12}$) the canted phase is suppressed and hysteresis involves collinear phases only. Magnetization curves in Fig. 2 demonstrate experimentally observed[4,5] features, such as inclined segments and horizontal plateaus.

4. Regions of hysteresis for fixed values of anisotropy

In this section we look at hysteresis behavior in more detail. We fix the anisotropy β and the FM–AFM exchange J_0 and study the state of the system as a function of parameters J, H (Fig. 4). We rewrite expressions (4), (7), (8) for the collinear-canted transition lines in the form $J = J(H, \beta, J_0)$

$$J_1 = -\frac{(H+\beta)(H+J_0+\beta)}{(2H+J_0+2\beta)}, \tag{15}$$

$$J_3 = \frac{(H-\beta)(H+J_0-\beta)}{(2H+J_0-2\beta)}, \tag{16}$$

$$J_5 = -\frac{(H-\beta)(H+J_0+\beta)}{(J_0+2\beta)}, \tag{17}$$

for the $\uparrow\uparrow$ phase (line A_1 in Fig. 4), the $\downarrow\downarrow$ phase (line A_3), and the $\uparrow\downarrow$ phase (line A_5), respectively. Lines J_1, J_3 cross at the point $H = -J_0/2$, $J = J' = J_0^2/8\beta - \beta/2$.

$$[(H+J_0)\cos\varphi_1 + 2\beta\cos^2\varphi_1 - \beta](H\cos\varphi_2 + 2\beta\cos^2\varphi_2 - \beta)$$
$$+[(H+J_0)\cos\varphi_1 + 2\beta\cos^2\varphi_1 + H\cos\varphi_2 + 2\beta\cos^2\varphi_2 - 2\beta]$$
$$\times J\cos(\varphi_1 - \varphi_2) = 0, \tag{18}$$

where the angles φ_i are not known explicitly. Eqs. (9), (10), and (18) give the dependence $J_3 = J(H)$ to describe the right boundary of the hysteresis loop (see line A_2 in Fig. 4). From Eq. (18) it follows that for fixed anisotropy β there exists a maximum value of the exchange constant J for which hysteresis takes place. It corresponds to $H = -J_0/2$ and

$$J = J'' = J_0^2\left(1 + \sqrt{1 + 32\beta^2/J_0^2}\right)/16\beta + \beta/2.$$

In the limit of a large enough exchange interaction ($J \sim 1/\beta$) at the right boundary of the hysteresis loop we obtain $\varphi_1 \approx \pi - \varphi_2 \approx \arccos(2\beta/J_0)$, $M \approx 8(\beta/J_0)^2$, and the right boundary of the hysteresis loop (line A_2 in Fig. 4) is given by $J \approx J'' - (J_0/\beta)\,(H + J_0/2)/4$.

The curves A_i in this figure determine the regions of existence of different structures of the FM system, and the hysteresis loops are located between lines A_1A_2 and A_4A_3.

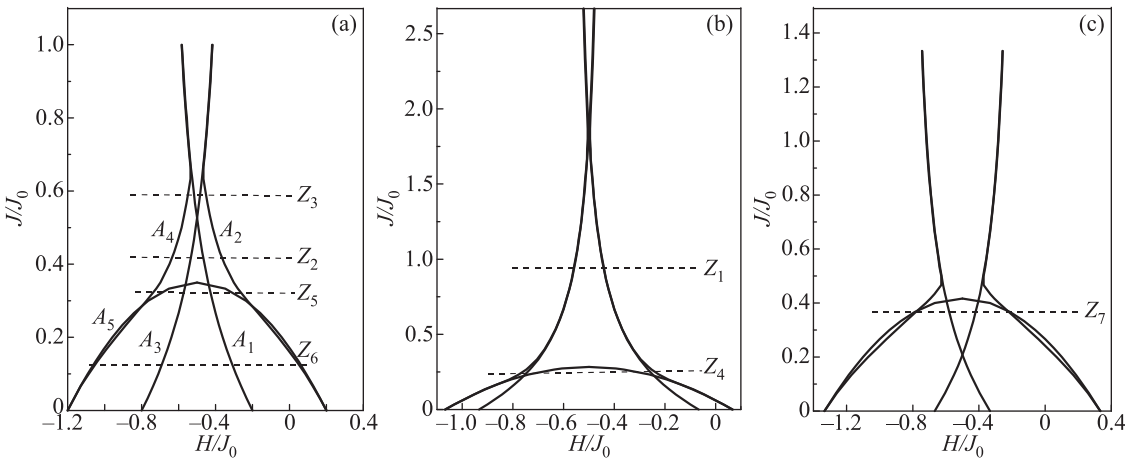

FIG. 4. Regions of hysteresis in the plane of the parameters $(J/J_0, H/J_0)$ for fixed values of anisotropy β: $\beta/J_0 = 0.2$ (a), 0.066 (b), and 0.33 (c).

In Fig. 4 domain of stability of the parallel phase (↑↑) is situated to the right of curve A_1, which starts at point $H=-\beta$ in the limit $J\to 0$ and asymptotically approaches infinity as $H\to -J_0/2-\beta$. The domain of stability of the parallel phase (↓↓) is located on the left of curve A_3, which starts at point $H=-J_0+\beta$ and asymptotically tends to infinity as $H\to -J_0/2+\beta$. The region below curve A_5 (which lies between points $H=-J_0-\beta$ and $H=\beta$) corresponds to the antiparallel phase (↑↓). Finally, the triangular area between the curves A_1, A_3, A_5 corresponds to the canted phase. For the fixed anisotropy parameter, the shape of the hysteresis loop changes with a change in parameter J.

For the point Z_2 (see Fig. 4) the hysteresis loop splits into two loops (Fig. 2, Z_2). For the line A_5 (with $J<J_0+2\beta$) we observe the plateau of the antiparallel phase (↑↓) in the $M(H)$ dependence (Fig. 2, Z_5). Upon further decrease in exchange interaction, this plateau occupies the entire region between the hysteresis loops (Z_6), but the canted phase still remains inside each of the two hysteresis loops. If magnetic anisotropy is small enough (Fig. 4(b)), there exists a domain of parameter J, for which there is no hysteresis (in contrast to FM systems without exchange bias).

5. The case of different anisotropy constants for the two FM layers ($\beta_1\neq\beta_2$)

We now briefly consider the case where $\beta_1\neq\beta_2$, i.e., the case of different anisotropy constants for the two layers of the ferromagnet. This simulates the presence of surface anisotropy arising due to broken lattice symmetry at the FM/AFM interface. Eqs. (4), (7), and (8) for the boundary of stability of various collinear phases change into

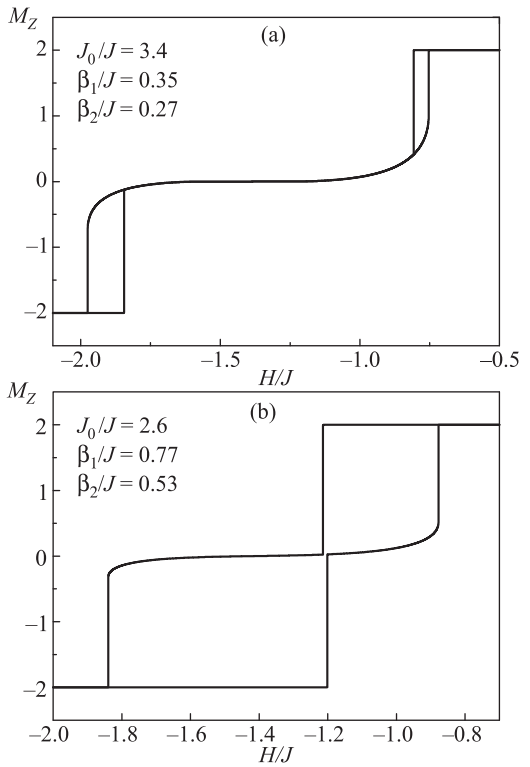

FIG. 5. Two typical magnetization curves $M(H)$ for the case $\beta_1\neq\beta_2$.

$$H_{\uparrow\uparrow}=-\frac{1}{2}(2J+J_0+\beta_1+\beta_2)+\frac{1}{2}\sqrt{4J^2+(J_0+\beta_1-\beta_2)^2}, \tag{19}$$

$$H_{\downarrow\downarrow}=-\frac{1}{2}(-2J+J_0+\beta_1+\beta_2)-\frac{1}{2}\sqrt{4J^2+(J_0-\beta_1+\beta_2)^2}, \tag{20}$$

$$H_{\uparrow\downarrow}=-\frac{1}{2}(J_0+\beta_1-\beta_2)+\frac{1}{2}\sqrt{(J_0-\beta_1-\beta_2)^2+2J_0(\beta_1+\beta_2)+J_0^2-4JJ_0-4J_0^2}, \tag{21}$$

respectively. The number of different possible types of the $M(H)$ curves for this is extremely large. We do not attempt a complete classification here, instead in Fig. 5 we present two typical $M(H)$ curves with $\beta_1\neq\beta_2$. One can easily see that the dependence $M(H)$ is no longer antisymmetric under the transformation $H\to -J_0-H$. In other words, for $\beta_1\neq\beta_2$ asymmetric hysteresis loops are observed. This demonstrates on the qualitative level that the presence of surface anisotropy at the FM/AFM interface leads to an asymmetric hysteresis loop, an experimentally observed feature of exchange bias systems.

Conclusion

In the present paper we have studied both analytically and numerically the hysteresis phenomenon in a FM/AFM bilayer in the framework of the "two-spin model" (two ferromagnetic layers in contact with a hard antiferromagnet). Twelve different types of magnetization curves $M(H)$ (both with and without hysteresis) were found for different values of parameters in the system (J_0/J and β/J). Explicit expressions for the boundaries of respective regions of the (J_0/J, β/J) plane were obtained.

Also the case of different anisotropy constants for the two ferromagnetic layers (surface anisotropy) was considered. Asymmetric $M(H)$ curves were obtained in this case. Despite the simplicity of the model, it is able to reproduce many experimentally observed features of the exchange bias phenomenon.

Financial support Complex program NASU through the Grant "Fundamental problems of nanostructural systems, nanomaterials and nanotechnologies" is gratefully acknowledged.

[a)]Email: pankratova_mari@mail.ru

[1]W. H. Meiklejohn and C. P. Bean, Phys. Rev. **102**, 1413 (1956).
[2]J. Nogues and I. K. Schuller, J. Magn. Magn. Mater. **192**, 203 (1999).
[3]A. E. Berkowitz and K. Takano, J. Magn. Magn. Mater. **200**, 552 (1999).
[4]D. N. Merenkov, A. N. Bludov, S. L. Gnatchenko, M. Baran, R. Szymchak, and V. A. Novosad, Fiz. Nizk. Temp. **33**, 1260 (2007) [Low Temp. Phys. **33**, 957 (2007)].
[5]S. L. Gnatchenko, D. N. Merenkov, A. N. Bludov, V. V. Pishko, Yu. A. Shakhaeva, M. Baran, R. Szymchak, and V. A. Novosad, J. Magn. Magn. Mater. **307**, 263 (2006).
[6]M. Kiwi, J. Magn. Magn. Mater. **234**, 584 (2001).
[7]M. D. Stiles and R. D. McMichael, Phys. Rev. B **59**, 3722 (1999).

[8]U. Nowak, K. D. Usadel, J. Keller, P. Miltényi, B. Beschoten, and G. Güntherodt, Phys. Rev. B **66**, 014430 (2002).
[9]T. C. Schulthess and W. H. Butler, Phys. Rev. Lett. **81**, 4518 (1998).
[10]J. Chen, G. Jin, and Y.-q. Ma, J. Phys.: Condens. Matter **19**, 236225 (2007).
[11]A. G. Grechnev, A. C. Kovalev, and M. L. Pankratova, Fiz. Nizk. Temp. **35**, 670 (2009) [Low Temp. Phys. **35**, 526 (2009)].
[12]A. G. Grechnev, A. C. Kovalev, and M. L. Pankratova, Fiz. Nizk. Temp. **35**, 603 (2009) [Low Temp. Phys. **35**, 476 (2009)].
[13]A. S. Kovalev and M. L. Pankratova, Fiz. Nizk. Temp. **37**, 1085 (2011) [Low Temp. Phys. **37**, 866 (2011)].

This article was published in English in the original Russian journal. Reproduced here with stylistic changes by AIP.